The Journal of Chemical Physics

RESEARCH ARTICLE | JULY 15 2022

Small ionic radii limit time step in Martini 3 molecular dynamics simulations

Balázs Fábián ; Sebastian Thallmair ; Gerhard Hummer

J. Chem. Phys. 157, 034101 (2022)
https://doi.org/10.1063/5.0095523

The Journal of Chemical Physics ARTICLE scitation.org/journal/jcp

Small ionic radii limit time step in Martini 3 molecular dynamics simulations

Cite as: J. Chem. Phys. **157**, 034101 (2022); doi: 10.1063/5.0095523
Submitted: 11 April 2022 • Accepted: 23 June 2022 •
Published Online: 15 July 2022

Balázs Fábián,[1,a)] Sebastian Thallmair,[2] and Gerhard Hummer[1,3]

AFFILIATIONS

[1] Department of Theoretical Biophysics, Max Planck Institute of Biophysics, Max-von-Laue Straße 3, 60438 Frankfurt am Main, Germany
[2] Frankfurt Institute for Advanced Studies, Ruth-Moufang-Straße 1, 60438 Frankfurt am Main, Germany
[3] Institute of Biophysics, Goethe University Frankfurt, 60438 Frankfurt am Main, Germany

[a)] **Author to whom correspondence should be addressed:** balazs.fabian@biophys.mpg.de

ABSTRACT

Among other improvements, the Martini 3 coarse-grained force field provides a more accurate description of the solvation of protein pockets and channels through the consistent use of various bead types and sizes. Here, we show that the representation of Na^+ and Cl^- ions as "tiny" (TQ5) beads limits the accessible time step to 25 fs. By contrast, with Martini 2, time steps of 30–40 fs were possible for lipid bilayer systems without proteins. This limitation is relevant for systems that require long equilibration times. We derive a quantitative kinetic model of time-integration instabilities in molecular dynamics (MD) as a function of the time step, ion concentration and mass, system size, and simulation time. We demonstrate that ion–water interactions are the main source of instability at physiological conditions, followed closely by ion–ion interactions. We show that increasing the ionic masses makes it possible to use time steps up to 40 fs with minimal impact on static equilibrium properties and dynamical quantities, such as lipid and solvent diffusion coefficients. Increasing the size of the bead representing the ions (and thus changing their hydration) also permits longer time steps. For a soluble protein, we find that increasing the mass of tiny beads also on the protein permits simulations with 30-fs time steps. The use of larger time steps in Martini 3 results in a more efficient exploration of configuration space. The kinetic model of MD simulation crashes can be used to determine the maximum allowed time step upfront for an efficient use of resources and whenever sampling efficiency is critical.

INTRODUCTION

Compared to its predecessors,[1,2] the recent Martini 3 force field[3] constitutes a significant advance in biomolecular simulations. Martini 3 offers consistently parameterized coarse-grained (CG) interaction sites of different sizes and a better coverage of the chemical space by a whole range of new bead types. This results in an improved representation of the molecular shape, packing, and interactions in general. The diversity of the ion models was strongly increased, now featuring five bead types Q1–Q5 in three resolutions ranging from "tiny" (T, 2-to-1 mapping) via "small" (S, 3-to-1 mapping) to "regular" (R, 4-to-1 mapping) beads. The parameterization of the beads features a Martini Hofmeister series from hard, more inorganic ions (Q5) to soft, more organic ions (Q1). In addition, specific interactions (e.g., those of cation-π type) can be incorporated using labels that were previously only available in the polarizable version.[4] The new features of Martini 3 resulted in a change in the resolution of hard ions, such as Na^+ and Cl^-, which are routinely added to biomolecular simulation systems to establish physiological conditions in terms of ionic strength. The size of both Na^+ and Cl^- ions changed from R to T, which means that in Martini 3, the ions are modeled without a hydration shell. This is in contrast to Martini 2, where a hydration shell was considered to be included in the larger R-bead type used for Na^+ and Cl^-.

While Martini 2 simulations were routinely run with a time step of $\Delta t = 30$ fs[5–7] according to the recommendation of the *new-rf* parameter set,[8] the currently recommended time step is $\Delta t = 20$ fs, which was used for all test systems during the parameterization of the force field. In several previous studies employing Martini 2, even $\Delta t = 40$ fs was used.[2,9,10] However, this was deemed excessive by the developers of the model,[11] and the use of such large time steps is generally discouraged.

Here, we show that the representation of Martini 3 ions as "tiny" charged beads of type TQ5 requires an integration time step no larger than 25 fs. For $\Delta t > 25$ fs, the tendency of the time integration to become unstable and crash the simulations increases significantly. We develop a quantitative kinetic model of the rate of crashing as a function of the integration time step, ion concentration, and ionic mass. By fitting the three parameters of this model globally to the observed crash statistics of the molecular dynamics (MD) runs, we identify ion–ion and ion–water interactions as the main culprits. We explore two possible solutions that permit simulations to run with larger time steps: by modifying the ionic mass and by changing the bead type of the ions. While the former keeps the desired resolution with almost no perturbations to the system, the latter is consistent with the multi-resolution approach of Martini 3. The effects and trade-offs made by these solutions are evaluated and discussed in detail. Moreover, the statistical model employed here to estimate the rate of crashing can be applied to determine an optimal time step for MD-based high-throughput campaigns. With integration stability being the major factor limiting the time step size, the general formalism used here to determine the maximum allowed time step should prove useful for an efficient deployment of resources and whenever sampling efficiency is critical in MD simulation.

THEORY

Altering the mass or bead type

In classical MD simulations, Newton's equations of motion (usually augmented with thermostats and barostats) are integrated numerically with finite time steps. The integration time step Δt is chosen in a trade-off between accuracy, e.g., to conserve the total energy, and the computational efficiency of sampling configuration space. To maximize efficiency, the time step is commonly chosen close to the stability limit of time integration.[12] For classical non-polarizable models, this limit is determined by the fastest molecular motions, in particular the rattling of stiff covalent bonds and tight non-covalent interactions, and the hard collisions between molecules on highly anharmonic potential surfaces.

For NaCl solutions and lipid bilayers, we observed that Martini 3 MD simulations required shorter time steps than in equivalent setups simulated with the Martini 2 model. As the main culprit, we identified the newly introduced ions modeled as "tiny" charged (TQ5) beads and their ion–ion interactions. As possible remedies, we consider (i) changing the ionic masses and (ii) changing the bead type from tiny to small (SQ5) or regular (RQ5).

The motivation behind changing the ionic mass is the invariance of Newton's equations of motion under a uniform scaling of all masses and of time by α and $\sqrt{\alpha}$, respectively. Whereas scaling all particle masses does not improve configuration space sampling, we expect that increasing the ionic mass will permit a longer time step. The displacements of heavier ions at each time step are smaller, which should reduce the risk of an uncontrolled clash, causing an instability in the numerical time integration. If such ion displacements limit the time step, we expect that the maximum allowed time step for stable time integration scales with the ionic mass m as

$$\frac{\Delta t'}{\Delta t} \approx \sqrt{\frac{m'}{m}}, \tag{1}$$

where we ignored the motions of the other particles. Then, starting from a time step $\Delta t = 20$ fs, doubling and quadrupling the ionic mass m would make it possible to use $\Delta t' = 30$ and 40 fs, respectively.

Importantly, changes in particle mass leave the equilibrium structural properties unchanged because the classical mechanical partition function separates into kinetic and configurational contributions. However, the dynamics of the system is generally modified in a nontrivial manner. Nevertheless, with a longer time step, one can expect a faster sampling of the relevant configuration space for the molecules with unmodified masses.

In Martini simulations, usually only relatively slow diffusive motions are of interest because the fast intramolecular and collision dynamics is impacted significantly by coarse-graining. Translational and rotational diffusion are dominated by hydrodynamic effects, as reflected in the Stokes–Einstein theory of 3D diffusion[13] and in the Saffman–Delbrück theory of 2D diffusion in lipid bilayers embedded in a 3D solvent.[14] Both theories predict that the diffusion coefficient of a dissolved molecular species does not depend directly on its mass, only on its size and the viscosity of the surrounding medium. Therefore, we expect that ionic mass changes have minimal impact on the diffusive dynamics.

Nevertheless, changes in the mass of some of the particles can potentially change the viscosity of the aqueous solvent and the membrane. Here, we consider increasing the mass of the ions described by TQ5 beads, leaving all other masses untouched. Importantly, these particles constitute only a tiny fraction of the molecules in the aqueous solvent and do not enter within the lipid bilayers. Therefore, we expect that doubling their mass will have only a very limited effect on the viscosity of the solvent and membrane and thus, in turn, on the diffusive dynamics of all species, including the ions themselves. We test this assumption by monitoring the diffusivity of the solvent and lipid species as a function of ionic mass. We keep the box dimensions constant in this comparison and do not correct for the large finite size effects in the computed diffusion coefficients.[15,16]

Modification of the bead type of the ions is based on the notion that in Martini 3, a change in the bead size of the ions represents a change in their hydration. Bead-size changes (accompanied by the corresponding changes in mass) are thus consistent with the coarse-graining philosophy of the force field (see the supplementary material of the original Martini 3 paper[3]). Moreover, the current resolution of lipid head groups, such as the choline moiety of phosphatidyl-choline (PC) lipids, is already low due to the employed 6-1 mapping,[2,17] where six non-hydrogen atoms are grouped together into a single interaction site. Therefore, adequate modeling of protein-less bilayers currently does not require a high resolution of the ions. We thus expect that an increase in the ion bead size will not significantly perturb the membrane properties.

Crash probability as a function of the time step

In the following, we develop a kinetic model of the probability that a simulation with a given time step will crash during a given total simulation time. We assume that, rarely, the position updates in time

integration place particles within a strongly repulsive region of the potential surface such that the subsequent force evaluation leads to numerical instabilities either immediately or after a few uncontrolled further integration steps.

Let Δt be the integration time step. With v the velocity in one dimension, the corresponding displacement is then $\Delta x = v\Delta t$, ignoring the higher-order acceleration terms. We now assume that displacements $\Delta x > \Delta x_{\text{crit}}$ are critical and lead to crashes. The velocities of a particle of mass m at inverse temperature β satisfy a Maxwell–Boltzmann distribution, $p(v)dv = \exp(-\beta m v^2/2)\sqrt{\beta m/(2\pi)}dv$. The probability of a critical displacement during a simulation time step becomes

$$P(\Delta x > \Delta x_{\text{crit}}) = \int_{\Delta x_{\text{crit}}/\Delta t}^{\infty} dv\, \exp(-\beta m v^2/2)\sqrt{\beta m/(2\pi)} \approx \frac{\gamma \Delta t\, \exp(-1/(2\gamma^2\Delta t^2))}{\sqrt{2\pi}}, \quad (2)$$

with $1/\gamma^2 = \beta m \Delta x_{\text{crit}}^2$. Here, we used the asymptotic expansion of the complementary error function. In a simulation system, we expect that a certain fraction $\sqrt{2\pi}f$ of the particle displacements (here, those of the "tiny" ions and their interaction partners) can result in such catastrophic clashes. The probability $Q = \sqrt{2\pi} f P(\Delta x > \Delta x_{\text{crit}})$ of a catastrophic displacement in a given time step is approximately

$$Q = f\gamma\Delta t\, \exp(-1/(2\gamma^2\Delta t^2)). \quad (3)$$

Assuming uncorrelated events and $0 < Q \ll 1$, the probability that a simulation run of n time steps will not crash is

$$P = (1-Q)^n \approx \exp\left[-tf\gamma\, \exp(-1/(2\gamma^2\Delta t^2))\right], \quad (4)$$

with $t = n\Delta t$ the total time. The crash times are thus predicted to be distributed exponentially, $p(t_{\text{crash}})dt_{\text{crash}} = k_{\text{crash}} \exp(-k_{\text{crash}} t_{\text{crash}})dt_{\text{crash}}$, with a rate that depends on the simulation time step as

$$k_{\text{crash}}(\Delta t) = f\gamma\, \exp(-1/(2\gamma^2\Delta t^2)) = k_{\text{crash}}^0\, \exp(-1/(2\gamma^2\Delta t^2)). \quad (5)$$

The crash rate has two parameters, f and γ, whose product defines $k_{\text{crash}}^0 = f\gamma$. In our systems, we expect that the dimensionless factor f depends on the concentration c_{ion} of ions as $f = (a{c_{\text{ion}}}^2 + bc_{\text{ion}})V$, with coefficients a and b, and V the system volume. Based on the definition and consistent with Eq. (1), we expect γ to depend on the mass of the ions approximately as $\gamma \propto 1/\sqrt{m}$.

METHODS

Simulation of NaCl solutions

To demonstrate the effect of changing ionic masses (or the lack thereof) on the viscosity μ_f of the fluid surrounding the bilayer, we prepared water boxes with 0, 0.075, 0.15, and 0.3M NaCl concentrations using *insane.py*[17] and the option -salt. All cubic boxes had an initial edge length of 10 nm. We simulated these NaCl solutions with the standard Martini 3 CG force field[3] and the Gromacs package[18] (version 2020.1). To eliminate differences stemming from finite size effects between these systems,[15] we took the smallest box as reference and removed the appropriate number of molecules from all others. This procedure resulted in equilibrium box lengths between 8.93 and 8.97 nm for all NaCl solution systems. No corrections were applied to account for finite size effects on diffusion. At every concentration, we performed simulations with time steps of 20, 30, and 40 fs and using the original, doubled, and quadrupled ionic masses (denoted as 1 × m, 2 × m, and 4 × m, respectively) to systematically test the effects on the diffusion coefficient and therefore on the viscosity of the bulk medium. Following a short energy minimization using a steepest descent algorithm, every system was equilibrated during a 1 μs run with a time step of 20 fs. This was followed by 3 μs-long production runs using 20, 30, or 40 fs time steps. Coordinates were saved for analysis every 0.5 ns. The temperature of the systems was kept at 310 K using a velocity re-scale thermostat.[19] The pressure was maintained at 1 bar using an isotropic Parrinello–Rahman barostat[20] (p_{ref} = 1 bar and τ_p = 12 ps).

To gain insight into the origin of the simulation crashes, we performed a large number of additional simulations using various combinations of parameters and concentrations. These simulations are collected in Table S1. In this set, every simulation used the settings as described above but with a fixed number of desired steps ($n_{\text{steps}} = 10^8$) instead of fixed total simulation time and without trying to match the overall volumes. The majority of these simulations could not achieve the specified $n_{\text{steps}} = 10^8$, and the only observable extracted from them was the time of crashing, as described below. To reduce the statistical uncertainty in the evaluation of the crash rate, every simulation was repeated 40 times.

Simulation of DPPC bilayers

We also performed MD simulations of fully solvated DPPC bilayers containing Na^+ and Cl^- ions with the Martini 2 and Martini 3 CG force fields. The initial systems were prepared using *insane.py*.[17] All bilayers were constructed in an initial box of 18 × 18 × 18 nm^3 and solvated with 14 405 CG waters (pure W for Martini 3 and 10% WF antifreeze[2] for Martini 2). The equilibrium membrane area in the simulation boxes was about 17 × 17 nm^2, larger than ≈8 × 8 nm^2 used in the Martini 3 validation test. Every simulation system contained 0.15M NaCl, as added with *insane.py* using the flag -salt 0.15. We performed all simulations with Gromacs 2020.1 and used 20, 30, and 40 fs time steps. We simulated a Martini 2 membrane for reference and Martini 3 membranes using TQ5 (standard Martini 3), SQ5, and RQ5 (=Q5) beads as monovalent ions. Finally, we tested the effect of increasing the ionic mass by a factor of 2. The doubled mass corresponds to using the interactions of TQ5 along with the mass of RQ5. The abbreviated labels of the above lipid simulations are M2, M3(-TQ5), M3-SQ5, M3-RQ5, and M3-2×m, respectively. All membranes were energy minimized using a steepest descent algorithm and further minimized by running 50 ns trajectories using 5 fs time steps. This was followed by a 5 μs equilibration using a time step of 20 fs. Then, production runs of 10 μs were performed using 20, 30, and 40 fs time steps and writing the positions to disk every 0.5 ns. The temperature of the systems was kept at 310 K using a velocity re-scale thermostat.[19] The pressure of the systems was controlled in a semi-isotropic manner with a compressibility of 3×10^{-4} bar^{-1}. For the initial energy

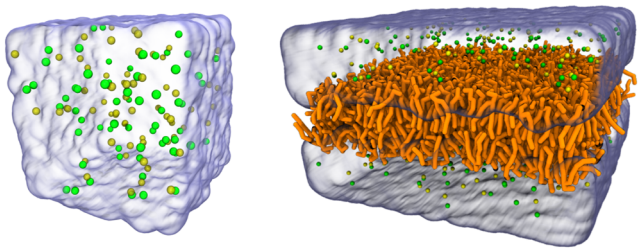

FIG. 1. Snapshots of the NaCl solution system (left) and the DPPC lipid bilayer system (right). Sodium and chloride ions are shown as yellow and green spheres and DPPC lipids as orange tubes. Water is represented as a transparent surface. The images were rendered using Visual Molecular Dynamics (VMD). [21]

minimization, we employed the Berendsen barostat[22] (p_{ref} = 1 bar and τ_p = 1 ps), while the equilibration and production proceeded with the Parrinello–Rahman barostat[20] (p_{ref} = 1 bar and τ_p = 12 ps). Figure 1 shows illustrative snapshots of the simulated NaCl solutions and lipid bilayers.

Analysis

In our numerical tests, we ran 40 simulations for each system, except for the shortest time steps (which resulted in consistently stable trajectories) and the longest time steps (which caused crashes almost immediately; see Table S1 for details). The time t_i is the targeted run length, $t_i = \Delta t \times 10^8$, if run i completed normally, or the time of the crash caused by an instability. For the exact definition of a crash, see Sec. 1.1 in the supplementary material. From the times t_i, we estimate the rate of crashing (and thus the reciprocal of the mean time to a crash) using a maximum-likelihood estimator for right-censored data and Poisson statistics,

$$k_{\text{crash}} = \frac{1}{t_{\text{crash}}} = \frac{n_{\text{crash}}}{\sum_{i=1}^{40} t_i}, \tag{6}$$

where $0 \le n_{\text{crash}} \le 40$ is the number of crashes observed in the 40 runs. We assessed the uncertainty of the estimator using the standard error $\sigma = k_{\text{crash}}/\sqrt{n_{\text{crash}}}$, which corresponds to the Cramér–Rao bound. This estimator gives us some guidance on the molecular factors causing the crashes. For instance, if ion–water interactions were dominant, we would expect $k_{\text{crash}} \propto c_{\text{ion}}$, where c_{ion} is the ion concentration. By contrast, if ion–ion interactions were dominant, we would expect $k_{\text{crash}} \propto (c_{\text{ion}})^2$, as discussed in the Theory section.

From the trajectories of the bulk NaCl solutions, we determined the diffusion coefficients D_{3D} of water. We computed the diffusion coefficients with an optimal Generalized Least Squares (GLS) estimator,[23] as implemented in the DiffusionGLS[24] package. The trajectories were unwrapped using a scheme that correctly takes into account volume fluctuations in the NPT ensemble,[25] as implemented in qwarp.[26]

We evaluated the properties of the membrane system using the same observables as in the validation of the original Martini 3 force field: area-per-lipid A_l, thickness d (both of them obtained with FATSLiM[27]), area compressibility modulus K_A (computed from the projected area fluctuations, without correction for finite size effects[28]), and S_n order parameter (using *do-order-gmx5.py*, available on the Martini website www.cgmartini.nl). In addition, we also calculated the density profile of the ions along the membrane normal and the lateral diffusion coefficient D_{lat} of the lipid centers of mass within the membrane.

RESULTS AND DISCUSSION

Stability of Martini 3 NaCl solution simulations as a function of the time step

We performed extensive MD simulations of the NaCl solutions at time steps between 20 and 40 fs and in a range of ion concentrations (see Table S1 for details). By computing the rate of crashing k_{crash} using Eq. (6), we found more frequent crashes at longer time steps and with the increasing number of ions, indicating an issue with the stability of the numerical time integration associated with the ions of bead type TQ5. To describe the time step dependence of these crashes, we fitted Eq. (5) to the k_{crash} values. As shown in Fig. 2, the slope of the curves in the semi-logarithmic representation is constant. Accordingly, a single γ parameter accurately captures the time-step dependence of the crash tendency independent of the ion concentration.

According to the theory, the prefactor $k^0_{\text{crash}} = f\gamma$ in Eq. (5) accounts for the ion concentration dependence. Indeed, the values of the dimensionless concentration factor $f = k^0_{\text{crash}}/\gamma$ obtained from the intercept of the fits in Fig. 2 exhibit a linear-quadratic concentration dependence on the ion concentration, as shown in Fig. 3. We incorporated this concentration dependence and the dependence on the overall system volume V into Eq. (5) in the form $k^0_{\text{crash}}(c_{\text{ion}}, V) = \gamma\left(ac^2_{\text{ion}} + bc_{\text{ion}}\right)V$. The time step, concentration, and volume dependent crash rate then becomes

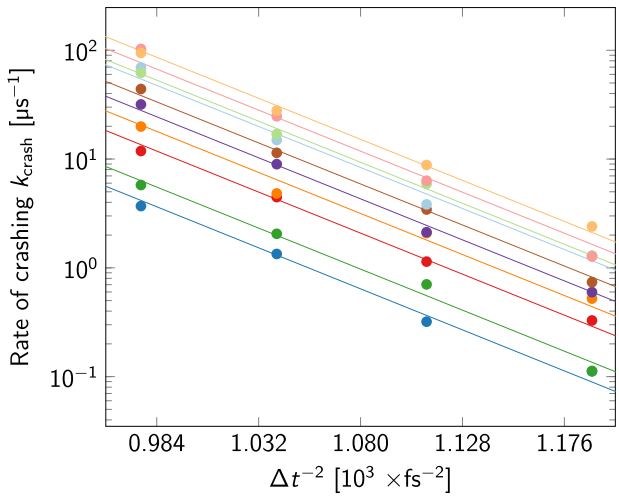

FIG. 2. Rate of crashing in the NaCl solutions as a function of the time step size. Shown is k_{crash} on a semi-logarithmic scale as a function of $1/\Delta t^2$. The individual colors correspond to fixed concentrations. The concentrations increase from the bottom curve (0.075M) to the top (0.5M). The solid lines represent fits of Eq. (5) using a common γ value.

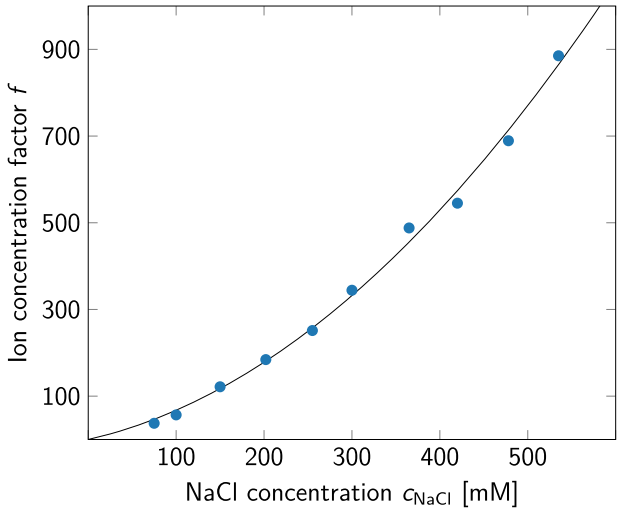

FIG. 3. Dependence of the rate of crashing on the ion concentration. Shown is the dimensionless concentration factor $f = k^0_{crash}/\gamma = (ac^2_{ion} + bc_{ion})V$, $c_{ion} = 2c_{NaCl}$ obtained from the intercept of the linear fits in Fig. 2 as a function of the ion concentration in NaCl solutions. The solid line shows a fit of a linear-quadratic dependence on c_{ion} with a fixed value of γ.

$$k_{crash}(c_{ion}, V, \Delta t) = \gamma\left(ac^2_{ion} + bc_{ion}\right)V \ \exp\left(-\frac{1}{2\gamma^2\Delta t^2}\right), \qquad (7)$$

where $a = 7.5820 \times 10^{-7}\,\mathrm{mM}^{-2}\,\mathrm{nm}^{-3}$, $b = 3.2043 \times 10^{-4}\,\mathrm{mM}^{-1}\ \mathrm{nm}^{-3}$, and $\gamma = 5.2568\ \mathrm{ps}^{-1}$. Note that a rearrangement of the prefactor gives $k^0_{crash}(c_{ion}, V) = \gamma n_{ions}(ac_{ion} + b)$, where n_{ions} is the total number of TQ5 ions in the system.

Equation (5) with a linear-quadratic concentration dependence accurately accounts for the observed crash rates k_{crash} across ion concentrations and time steps. As shown in Fig. 4, we achieved an excellent agreement between the numerical data for time steps between 29 and 32 fs and the simple 3-parameter theory. As a final validation, we varied the system size. As predicted by the theory, k_{crash} depends linearly on the overall volume of the system (see Fig. S1). Incorporating the concentration and system size dependence into Eq. (5) gives a general equation, Eq. (7), capable of predicting the expected number of crashes. The analysis presented here required a careful control of certain simulation parameters. In particular, we found that using a fixed value of Verlet buffer tolerance instead of a fixed neighbor list cut-off (rlist) effectively masked the functional form of the concentration dependence of k_{crash} (see Fig. S2).

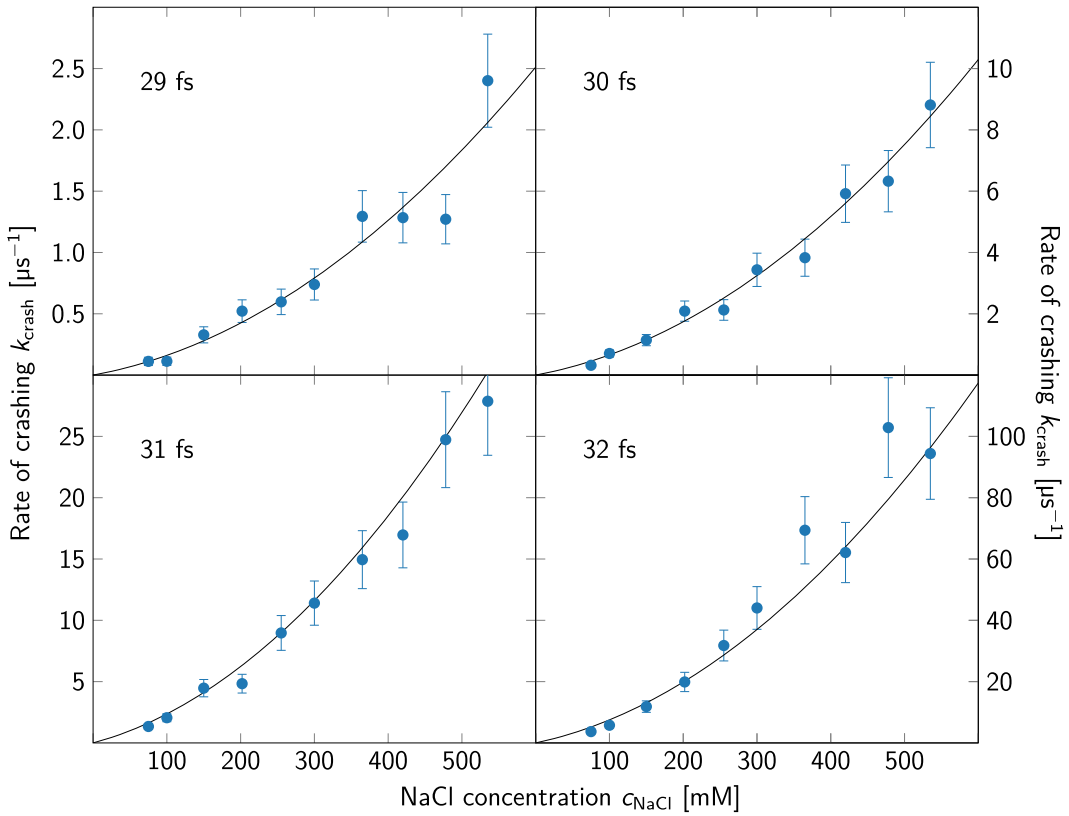

FIG. 4. Rate of crashing in the NaCl solutions as a function of the NaCl concentration analyzed for different time steps. The panels correspond to $\Delta t = 29$, 30, 31, and 32 fs. The solid black lines are fits of Eq. (6) with three parameters γ, a, and b. The error bars represent the standard error. Note that the y-scale varies between the panels and that $c_{ion} = 2c_{NaCl}$.

In addition to estimating the crash rate, our model also allows us to determine the particle types involved in the crashes. At physiological ion concentrations, $c_{NaCl} = c_{ion}/2 \approx 150$ mM, crashes are more likely to be caused by ion–water collisions than ion–ion collisions. According to the theory, their ratio is about $ac_{ion}/b \approx 0.71$. Supported by the data, the theory also predicts an extremely steep increase in k_{crash} as a function of the time step, which was also the main reason for the use of such a seemingly narrow range of Δt between 29 and 32 fs. With relatively short (10^8 steps) runs of a small (~6000 particles) test system, the theory predicts that one would have to perform ~10 000 s of simulation time at $\Delta t = 20$ fs to reach a single failure even in the most concentrated (500 mM) system. On the other extreme of the scale, $\Delta t = 40$ fs results in a failure after every ~500 steps (every 20 ps) on average. These numbers are supported by our observations in simulations using the respective time steps. As a practical example, we applied Eq. (7) to predict k_{crash} in a system of 150 mM NaCl solution consisting of 10^5 particles corresponding to a cubic box of edge length ~23 nm. The estimated k_{crash} as a function of the time step is presented in Fig. 5. Using $\Delta t = 25$ fs, one can expect one crash about every 366 μs of simulation time, while $\Delta t = 26$ fs already results in a crash every 41 μs. We expect that the addition of proteins or a lipid bilayer to the systems does not fundamentally alter k_{crash}, provided that they do not introduce additional numerical instabilities. As a consequence, our scaling law limits the largest accessible time step to $\Delta t \leq 25$ fs in any practical application.

Increased ionic mass stabilizes time integration

In numerical tests of the NaCl solutions, we found that an increase in the mass of the ions described by TQ5 beads resulted in more stable time integration. According to Eq. (1), we expect that increasing the ionic masses by a factor of $(m'/m)^2 = 40^2/30^2 \approx 1.7778$ will allow us to use a time step longer by a factor of 4/3.

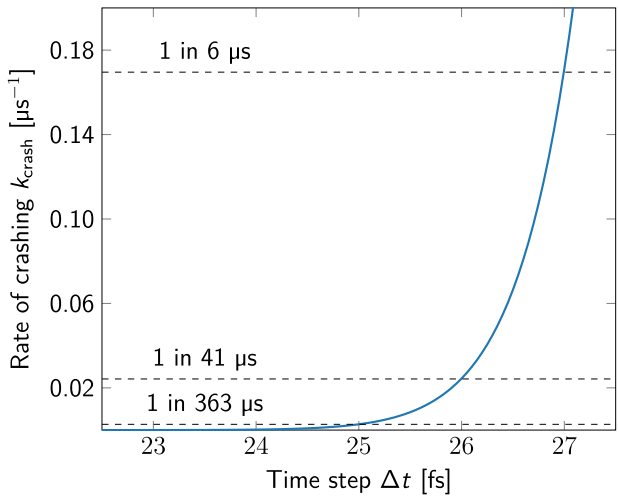

FIG. 5. Rate of crashing in a 150 mM NaCl solution consisting of 10^5 CG beads, as estimated using Eq. (7). Horizontal lines indicate k_{crash} for runs with time steps of $\Delta t = 25$, 26, and 27 fs (bottom to top). The lines are labeled by the expected mean time to a first crash.

In the more elaborate model [Eq. (5)], the ionic mass m enters through γ. For a modified ionic mass m', we have $\gamma' = \gamma\sqrt{m/m'}$. In practice, the mass m' may have to be adjusted to account for the more complex coupled motions of the different particles. As shown in Fig. S3, we obtain excellent agreement of the crash rate predicted using Eq. (5) with the data obtained for the heavier ions by using an effective mass of $m' = 1.7188m$ instead of the nominal ionic mass of $1.7778m$, which amounts to a difference of around 3.5%.

These findings further confirm that the ions of TQ5 type indeed determine the stability of the NaCl solutions. Moreover, they also demonstrate that an ionic mass increase improves the stability by allowing a time step scaled approximately by the square root of ionic masses after and before mass correction, in close agreement with the prediction of Eq. (1). Taking the 0.3M test system as an example, doubling the masses at $\Delta t = 30$ fs reduces the estimated crash rate k_{crash} from $\approx 10/\mu s$ to $\approx 10^{-8}/\mu s$, while quadrupling the masses at $\Delta t = 40$ fs reduces the estimated k_{crash} from $\approx 10^5/\mu s$ to $\approx 10^{-10}/\mu s$.

Multivalent metal ions play an important role in biology. For reference, we simulated systems containing concentrated $CaCl_2$ using the same protocol as above (see Table S2) to test if the presence of Ca^{2+} ions limits the allowable time steps. In Martini 3, Ca^{2+} ions are represented as "small" beads. In our tests, we found that changes in the mass of the "tiny" Cl^- stabilized the time integration, implying that the "small" Ca^{2+} ions are not causing integration instabilities. We conclude that ion size, not ion charge, is the dominant factor restricting the allowable time step.

Increased ionic masses leave the structure of NaCl solutions unchanged and minimally impact their dynamics

To investigate the perturbations caused by an increase in ionic masses, we analyzed the structure and dynamics of the NaCl solutions. As expected, the modification of the ionic masses does not impact the structural properties (Fig. S7). We found the ion–ion radial distribution functions (RDFs) to be independent of the integration time step and the ionic mass. The diffusion coefficients D_{3D} of CG water obtained from these systems are collected in Table I. The data confirm our expectations based on hydrodynamic considerations:[13,14] changing the mass of the ions has only small effects on the diffusion coefficient for a given time step. At a NaCl concentration of 300 mM, a four-fold increase in ionic mass reduced the water diffusivity by about 2%. We expect that the ionic mass will impact the librational motion; however, these non-diffusive motions occur on timescales below the frequency of sample collection (Fig. S4). The observed decrease in diffusivity with the increasing NaCl concentration is in agreement with the tendency observed in experiments.[29] However, we also noticed a mass-independent small decrease in D_{3D} with increasing time step Δt. When compared to the conventional approach of fitting a straight line to an *ad hoc* interval of the MSD curve, the D_{3D} values calculated with a GLS estimator show smaller errors, more consistent estimates between replicas and clearer tendencies across the simulations (see Table S4 along with Figs. S4 and S6 in the supplementary material). Therefore, care must be taken not only when one compares diffusion coefficients from simulations

TABLE I. Estimated D_{3D} diffusion coefficient (nm^2/ns) of the CG water beads in Martini 3 NaCl solutions at various ion concentrations. The results are listed for ionic masses multiplied by factors 1, 2, and 4 and for time steps of 20, 30, and 40 fs. The errors are smaller than 0.01 nm^2/ns. These values were obtained from the correctly unwrapped trajectories[25] using DiffusionGLS.[23,24] Entries are missing where simulations suffered from a high rate of crashing k_{crash}. The results are listed without corrections for finite system size.[15]

	0.0M	0.075M			0.15M			0.3M		
	1 × m	1 × m	2 × m	4 × m	1 × m	2 × m	4 × m	1 × m	2 × m	4 × m
20 fs	2.43	2.26	2.25	2.25	2.11	2.10	2.08	1.81	1.80	1.77
30 fs	2.28	2.15[a]	2.14	2.14	···	2.00	2.00	···	1.73	1.71
40 fs	2.10	···	1.99[a]	1.98	···	···	1.86	···	···	1.62

[a]These simulations had k_{crash} around $\mathcal{O}(1/\text{simulation})$

performed using different time steps but also when using different estimators.[23]

Ionic mass increase has no discernible effect on the structure and dynamics in lipid membrane systems

Having established the lack of appreciable effects of ionic mass in bulk aqueous solution, we turned our attention to the neat DPPC bilayers. As for NaCl solutions, missing entries in all subsequent tables indicate that a high crash rate made it impossible to obtain converged results. The average values of area-per-lipid A_l and membrane thickness d are collected in Tables II and III. DPPC lipids modeled with the standard Martini 3 model [denoted M3(-TQ5)] have a smaller A_l value and correspondingly higher d than in Martini 2 (M2), consistent with its parameterization. Doubling the mass of TQ5 (system M3-2×m) and subsequently increasing Δt have no detectable effect on either of these quantities.

The lipid models in Martini 3 are designed to be softer than those in Martini 2.[3] Correspondingly, DPPC lipids in the Martini 3 validation exhibited K_A values of 232.9 ± 13.3 mN/m, in excellent agreement with the experimentally measured value of 231 ± 20.0 mN/m.[30] The K_A values calculated in this work are collected in Table IV. Our values are also in general agreement with the experimental data but somewhat below them. The discrepancy is not surprising: K_A values are sensitive to both the length of the time steps[31] and system size,[31,32] consistent with our simulations. In particular, the dependence on system size originates from the difference between real and projected membrane areas due to the undulations of the membrane.[28] A word of caution is needed at this point: a common practice when simulating large patches of planar membranes is to apply weak harmonic restraints to a quarter of the lipids in one of the two leaflets.[16,33] Such "pinning" of a subset of lipids suppresses long wavelength undulations. The suppression of undulations should be taken into account when comparing K_A from simulations of different sizes. As we saw with A_l and d, doubling the ionic masses does not influence K_A. However, doubling Δt from 20 to 40 fs resulted in a noticeable decrease (10%–20%) in K_A for the M2 and M3-RQ5 systems, where runs with Δt = 40 fs were stable.

The lipid tail order parameter values S_n presented in Table V show a higher degree of order in Martini 3 than in the previous version. Because S_n is computed as an average over the bonds involving lipid tail beads, the values are unaffected by changes in the surrounding medium. An increase in Δt causes a minute increase in S_n, which matches our expectation of straighter lipid chains based on the computed membrane thickness values.

In addition to the properties used in the optimization of the Martini 3 force field, we calculated the density profile of the ions along the membrane normal and lateral diffusion coefficient D_{lat} of the lipid centers of mass. Similar to the radial distribution profiles of the NaCl solutions (Fig. S7), Fig. 6 demonstrates that the

TABLE III. Membrane thickness d (nm) from simulations of DPPC bilayers. The error is less than 0.025 nm. Entries are missing where simulations failed to run properly.

	M2	M3(-TQ5)	M3-SQ5	M3-RQ5	M3-2×m
20 fs	4.147	4.195	4.194	4.190	4.195
30 fs	4.151	···	4.202	4.198	4.203
40 fs	4.157	···	···	4.209	···

TABLE II. Average area-per-lipid A_l (Å^2) from simulations of DPPC bilayers. The error is less than ±0.5 Å^2. Entries are missing where simulations failed to run properly. M2 and M3 refer to Martini 2 and Martini 3, respectively.

	M2	M3(-TQ5)	M3-SQ5	M3-RQ5	M3-2×m
20 fs	60.6	59.7	59.7	59.8	59.7
30 fs	60.5	···	59.5	59.6	59.5
40 fs	60.4	···	···	59.4	···

TABLE IV. Area compressibility modulus K_A (mN/m) from simulations of DPPC bilayers. The error is less than 2 mN/m. Entries are missing where simulations failed to run properly. The results are listed without corrections for finite size.[28]

	M2	M3(-TQ5)	M3-SQ5	M3-RQ5	M3-2×m
20 fs	279	220	221	216	218
30 fs	254	···	197	197	204
40 fs	243	···	···	179	···

TABLE V. Average order parameter S_n of the carbon chains from simulations of DPPC bilayers. The error is less than 0.001. Entries are missing where simulations failed to run properly.

	M2	M3(-TQ5)	M3-SQ5	M3-RQ5	M3-2×m
20 fs	0.455	0.481	0.481	0.479	0.481
30 fs	0.457	···	0.485	0.483	0.485
40 fs	0.460	···	···	0.488	···

TABLE VI. Lateral diffusion coefficients D_{lat} (10^{-2} nm^2/ns) from simulations of DPPC bilayers. The error is smaller than 0.1 $\times 10^{-2}$ nm^2/ns. Entries are missing where simulations failed to run properly.

	M2	M3(-TQ5)	M3-SQ5	M3-RQ5	M3-2×m
20 fs	5.80	5.58	5.64	5.64	5.54
30 fs	5.69	···	5.54	5.49	5.46
40 fs	5.51	···	···	5.31	···

obtained density profiles are insensitive to changes in the ionic mass, which is also true for the separate density profiles of Na^+ and Cl^- (see Fig. S8).

Compared to Martini 2, the lateral diffusion coefficient D_{lat} of DPPC lipids decreased in Martini 3, consistent with the higher order of the lipid chains, as seen from Table VI. The GLS estimator again provided diffusion coefficients with smaller statistical errors and clearer tendencies (see Table S5 and Fig. S5 in the supplementary material). Note, however, that these diffusion coefficients were not corrected for finite-size effects.[16] From the computed D_{lat} values, it is clear that simply changing the mass of TQ5 beads without increasing Δt does not noticeably alter the diffusion coefficient of the lipids, which is in accord with our results for the NaCl solutions.

Bead type changes have minimal impact on the structure and dynamics of the membrane

As an alternative solution to changing the masses, one can modify the bead type used to represent ions in Martini 3. The use of SQ5 beads allowed us to increase Δt to 30 fs, meaning that not a single crash was detected in the 40 replicas of the NaCl solutions. However, the combination of SQ5 beads and Δt = 40 fs resulted in an average of 5 crashes per simulation. Further increasing the bead size to RQ5 made it possible to run simulations at Δt = 40 fs. The procedure of increasing the bead size is fully consistent with the Martini 3 philosophy, and it represents the inclusion of hydrating waters in the ionic bead. Just as in the case of mass changes, we assessed the differences that occur upon changing the bead type from TQ5 to SQ5 or RQ5.

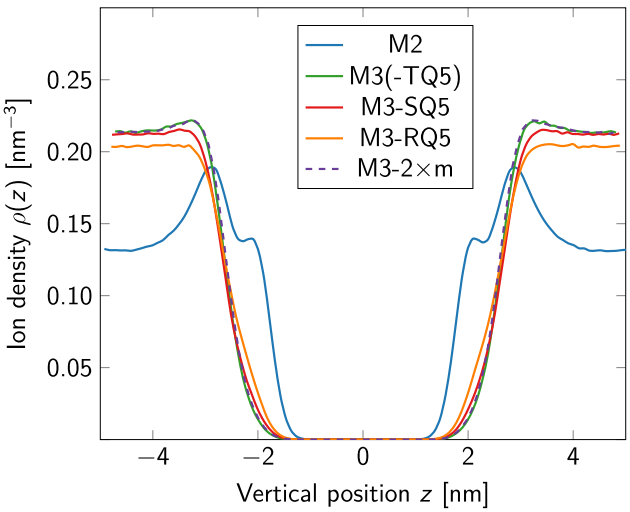

FIG. 6. Number density profile of ions along the direction normal to the DPPC membrane. The mid-plane of the bilayer is located at z = 0 nm. The results are shown for a time step Δt = 20 fs and are representative of all time steps.

The average values of A_l, d, and K_A are listed in Tables II–IV, respectively, in columns M3-SQ5 and M3-RQ5. Similar to changing the ionic mass, modifying the bead type while keeping Δt constant has virtually no effect on these values. Whereas increasing Δt does not affect A_l and d values, we found the K_A values to decrease noticeably by 10%–20%. Nevertheless, the changes introduced between Martini 2 and Martini 3 are largely preserved independent of the time step. Moreover, the lipid tail order parameters S_n in Table V are insensitive to the ionic bead type, while an increase in Δt produces an increase comparable to that observed in the system with doubled masses (also in Table V).

The modification of the bead type altered the distribution of ions around the membrane. However, as Fig. 6 shows, these changes are minor compared to those between the Martini 2 and 3 versions and between different atomistic force fields.[34] The alteration of the bead type also produced a detectable increase in the lipid diffusivity, indicating a somewhat more fluid liquid phase (Table VI). However, the effects of changing the time step Δt on lipid diffusion are larger than the effects of changing the ionic mass in the ranges considered.

To assess the impact of changing the ionic mass or the bead type in systems containing charged lipids or unsaturated lipid chains, we also tested DPPC bilayers containing 5% PI-(4,5)P_2 (C16:0/18:1 with phosphatidylinositol 4,5-bisphosphate head group)[35] and neat DIPS (di-C16:2-C18:2 with phosphatidylserine head group) bilayers using the Martini 3 force field. The results are presented in Tables S6 to S10 and Figs. S9 and S10 for the PI-(4,5)P_2-containing membranes and in Tables S11 to S15 and Fig. S11 for the neat DIPS membranes. The PI-(4,5)P_2-containing simulations were limited to a maximum time step of Δt = 30 fs. While the differences in the computed quantities of the PI-(4,5)P_2-containing membranes as a function of ion type were commensurate with those observed in our simulations of neat DPPC membranes, the properties of the neat DIPS bilayers showed somewhat larger changes with the ion bead type. By contrast, altering the ion masses did not have any significant impact on the membrane properties, irrespective of the membrane composition. We conclude that for highly charged membrane systems, the effect of modifying the ionic bead type must be carefully assessed, as it might affect relevant system properties, such as the gel–fluid melting temperature of the system.

Increase in "tiny" bead masses enables protein simulations at $\Delta t = 30$ fs

A remaining open question is if biomolecular systems containing proteins and lipid membranes can be simulated at $\Delta t = 30$ fs. To assess the possibility of using a time step of $\Delta t = 30$ fs in protein systems, we tested the stability of the soluble protein hen egg-white lysozyme (HEWL) at time steps larger than $\Delta t = 20$ fs. We did not observe any crashes for time steps up to $\Delta t = 28$ fs. To be able to run a simulation at $\Delta t = 30$ fs, we followed the same strategy as with the ions and increased the masses of the T ("tiny") beads in the protein to the default S ("small") bead mass of 54. This enabled stable simulations of HEWL with a time step of $\Delta t = 30$ fs without significantly affecting the structure of the protein. Details on the simulations and a comparison of the protein backbone root mean square fluctuations and ion occupancy are provided in the supplementary material (Sec. 15). We suggest to use increased T bead masses in proteins for the equilibration of the lipid membrane in mixed protein–lipid systems and to switch back to the original masses for rigorous production runs.

Energy conservation in Martini 3 simulations

The energy conservation in coarse-grained simulations has been the subject of intense debate.[11,36] To investigate the conservation of energy in Martini 3, we simulated an all-atom system consisting of 4139 TIP4P-D water molecules[37] (denoted as AA), a neat Martini 3 water box of the same volume (1050 water beads, denoted as CG-small), and another neat Martini 3 water box with the same number of beads (4139) as molecules in the all atom system (denoted as CG-large). Every simulation was performed in five replicas. After an initial equilibration at constant temperature, the simulations were continued for 5 ns without thermostatting, i.e., nominally at constant energy. Over this time, the total energy exhibited a linear drift. The total energies E_{total} are plotted as a function of the simulation time in Fig. 7. The corresponding energy drift values $\mathrm{d}E_{\text{total}}/\mathrm{d}t$ in Table S3 were estimated from the slope in straight-line fits. We found the energy drift values in the CG-small and CG-large systems to be nearly identical despite the difference in system size (see Table S3). Importantly, the energy drift in the coarse-grained systems is ~100-fold smaller than in the all-atom system even for a time step of 40 fs in the CG simulations. We attribute the more strict energy conservation to the smoothness of the potential energy function of coarse-grained force fields. However, a deeper investigation of this issue is beyond the scope of this study.

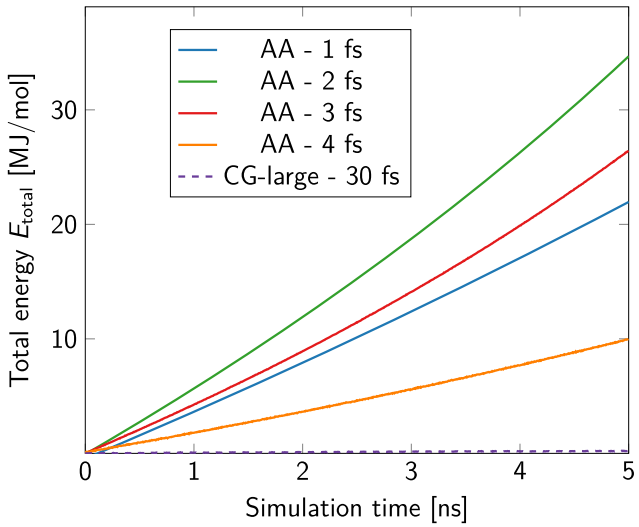

FIG. 7. Time course of the total energy E_{total} during a single, representative replica of the 5 ns long simulations. AA denotes the all-atom TIP4P-D water system and CG-large a neat Martini 3 water box that contains the same number of beads as the molecules in AA. The labels 1, 2, 3, 4, and 30 fs indicate the time steps. In the case of CG-large, only the 30 fs system is shown for clarity. See Table S3 for a list of the corresponding energy drifts.

CONCLUSIONS

The recently developed Martini 3 force field has successfully addressed several fundamental issues raised by Alessandri *et al.*[38] Most importantly, the introduction of specific cross-interaction terms between particles of different sizes created a consistent framework for the use of different bead sizes.

Here, we showed that the introduction of the "tiny" Martini 3 bead type for representing unhydrated Na^+ and Cl^- ions limits the accessible time step to below 25 fs. To achieve this, we performed extensive statistical analyses of the rate of crashing and developed a quantitative model of the crash rate $k_{\text{crash}}(c_{\text{ion}}, \Delta t, V)$. The model revealed the role of ion–ion and ion–water collisions in bringing about the crashes. The insight into the factors limiting the stability of MD time integration for neat NaCl aqueous solutions could be transferred to larger and more complex systems containing lipid bilayers. The knowledge of such stability limits greatly facilitates the rational design of computational experiments and the optimal use of available resources. A particular example is the free energy method of Lechner *et al.* relying on fast-switching trajectories, where the optimum efficiency of the algorithm was achieved using Δt just short of the stability limit.[12,39] Another example is the setup of *in silico* high throughput campaigns, such as the optimization of compositions of ionic liquids[40] or deep eutectic solvents[41] for liquid–liquid extractions, where the statistical model can be applied to determine an optimal time step for a given set of molecular systems.

Moreover, our simulations of NaCl solutions demonstrated that increasing the ionic mass has no significant effects on the structure or dynamics of the system (beyond the timescale of librational motions). Doubling (quadrupling) the masses allowed us to perform simulations at $\Delta t = 30$ fs (40 fs), but this resulted in somewhat slower diffusion. The properties of membrane systems containing DPPC lipids were also insensitive to doubling the mass. The larger time step had a minute effect on the structure of the bilayer, and the change in D_{lat} was even smaller than in the case of the NaCl solutions.

As an alternative consistent with the philosophy of Martini 3, we explored the impact of changing the size of the charged bead used to represent ions. Again, we noticed only a minor influence on the dynamical and structural properties of protein-less bilayers while making the use of an increased time step possible.

Increased ionic masses or altered bead types allowed us to use a time step of Δt = 30 fs (with SQ5) or 40 fs (with RQ5) to model protein-less bilayers. Increased time steps can provide crucial speed-up, e.g., for simulating phase separating lipid mixtures.[5,42] Although simulations of neat DPPC bilayers were running stably even at 40 fs, we do not recommend going beyond 30 fs. Major reasons to avoid time steps as long as Δt = 40 fs, besides the general consensus,[11] are the following: (i) the structural and dynamical properties of the system undergo relatively larger changes between 30 and 40 fs than between 20 and 30 fs as seen, e.g., in the diffusion coefficients of water in NaCl solutions; (ii) in the simulations of neat DPPC bilayers, only the M3-RQ5 system could tolerate such a high time step; (iii) the introduction of more finely mapped lipids, such as phosphatidylinositol 4,5-bisphosphate,[35] precludes the use of 40 fs (see the supplementary material). Our analysis indicated that to reach Δt = 30 fs, it suffices to either double the ionic mass or change the bead type to SQ5, which both have only a mild effect on the behavior of the system. Moreover, we showed that by increasing the T bead mass in proteins, it is also possible to simulate proteins using a time step of Δt = 30 fs.

Another known issue that limits the time step in three-component phase separating systems is the presence of insufficiently converged constraints.[43] We plan to address this problem in a future publication.

SUPPLEMENTARY MATERIAL

See the supplementary material for the definition of crash in simulations, the influence of rlist, doubling of masses, changing the volume, and Ca^{2+} on k_{crash}, the magnitude of total energy drift in all-atom and CG simulations, the diffusion coefficients obtained with the conventional estimator and its comparison with the GLS estimator, the ion–ion radial distribution functions in the NaCl solutions, the density profiles of ions around the DPPC membrane, the results concerning the PI-(4,5)P_2 containing membranes and neat DIPS membranes, and the results for a soluble protein.

ACKNOWLEDGMENTS

B.F. is grateful to Dr. Jakob Tómas Bullerjahn for fruitful discussions regarding statistical data analysis and to Dr. Jürgen Köfinger for insightful discussions on hydrodynamics. This research was supported by the Max Planck Society (B.F. and G.H.). S.T. and G.H. acknowledge the Center for Multiscale Modelling in Life Sciences (CMMS) sponsored by the Hessian Ministry of Science and Art for funding. S.T. acknowledges the Alfons und Gertrud Kassel Foundation and the Dr. Rolf M. Schwiete Foundation for funding.

AUTHOR DECLARATIONS

Conflict of Interest

The authors have no conflicts to disclose.

Author Contributions

Balázs Fábián: Conceptualization (equal); Data curation (equal); Investigation (lead); Visualization (lead); Writing – original draft (lead); Writing – review & editing (equal). **Sebastian Thallmair:** Conceptualization (supporting); Data curation (equal); Investigation (supporting); Visualization (supporting); Writing – original draft (supporting); Writing – review & editing (equal). **Gerhard Hummer:** Conceptualization (equal); Methodology (lead); Resources (lead); Writing – original draft (supporting); Writing – review & editing (equal).

DATA AVAILABILITY

The data that support the findings of this study are openly available on Zenodo at https://doi.org/10.5281/zenodo.6656149 (reference number 10.5281/zenodo.6656149).

REFERENCES

[1] S. J. Marrink, A. H. De Vries, and A. E. Mark, "Coarse grained model for semiquantitative lipid simulations," J. Phys. Chem. B **108**, 750–760 (2004).
[2] S. J. Marrink, H. J. Risselada, S. Yefimov, D. P. Tieleman, and A. H. De Vries, "The Martini force field: Coarse grained model for biomolecular simulations," J. Phys. Chem. B **111**, 7812–7824 (2007).
[3] P. C. T. Souza, R. Alessandri, J. Barnoud, S. Thallmair, I. Faustino, F. Grünewald, I. Patmanidis, H. Abdizadeh, B. M. H. Bruininks, T. A. Wassenaar *et al.*, "Martini 3: A general purpose force field for coarse-grained molecular dynamics," Nat. Methods **18**, 382–388 (2021).
[4] H. M. Khan, P. C. T. Souza, S. Thallmair, J. Barnoud, A. H. De Vries, S. J. Marrink, and N. Reuter, "Capturing choline–aromatics cation- π interactions in the MARTINI force field," J. Chem. Theory Comput. **16**, 2550–2560 (2020).
[5] M. D. Weiner and G. W. Feigenson, "Presence and role of midplane cholesterol in lipid bilayers containing registered or antiregistered phase domains," J. Phys. Chem. B **122**, 8193–8200 (2018).
[6] C. M. Rosetti, G. G. Montich, and C. Pastorino, "Molecular insight into the line tension of bilayer membranes containing hybrid polyunsaturated lipids," J. Phys. Chem. B **121**, 1587–1600 (2017).
[7] J. D. Perlmutter and J. N. Sachs, "Interleaflet interaction and asymmetry in phase separated lipid bilayers: Molecular dynamics simulations," J. Am. Chem. Soc. **133**, 6563–6577 (2011).
[8] D. H. De Jong, S. Baoukina, H. I. Ingólfsson, and S. J. Marrink, "Martini straight: Boosting performance using a shorter cutoff and GPUs," Comput. Phys. Commun. **199**, 1–7 (2016).
[9] C. Xing, O. H. S. Ollila, I. Vattulainen, and R. Faller, "Asymmetric nature of lateral pressure profiles in supported lipid membranes and its implications for membrane protein functions," Soft Matter **5**, 3258–3261 (2009).
[10] S. Jalili and M. Akhavan, "A coarse-grained molecular dynamics simulation of a sodium dodecyl sulfate micelle in aqueous solution," Colloids Surf., A **352**, 99–102 (2009).
[11] S. J. Marrink, X. Periole, D. P. Tieleman, and A. H. de Vries, "Comment on "On using a too large integration time step in molecular dynamics simulations of coarse-grained molecular models" by M. Winger, D. Trzesniak, R. Baron and WF van Gunsteren, Phys. Chem. Chem. Phys. 2009, 11, 1934," Phys. Chem. Chem. Phys. **12**, 2254–2256 (2010).
[12] W. Lechner, H. Oberhofer, C. Dellago, and P. L. Geissler, "Equilibrium free energies from fast-switching trajectories with large time steps," J. Chem. Phys. **124**, 044113 (2006).
[13] A. Einstein, "Über die von der molekularkinetischen Theorie der Wärme geforderte Bewegung von in ruhenden Flüssigkeiten suspendierten Teilchen," Ann. Phys. **4**, 549 (1905).
[14] P. G. Saffman and M. Delbrück, "Brownian motion in biological membranes," Proc. Natl. Acad. Sci. U. S. A. **72**, 3111–3113 (1975).
[15] I.-C. Yeh and G. Hummer, "System-size dependence of diffusion coefficients and viscosities from molecular dynamics simulations with periodic boundary conditions," J. Phys. Chem. B **108**, 15873–15879 (2004).

[16]M. Vögele, J. Köfinger, and G. Hummer, "Hydrodynamics of diffusion in lipid membrane simulations," Phys. Rev. Lett. **120**, 268104 (2018).
[17]T. A. Wassenaar, H. I. Ingólfsson, R. A. Böckmann, D. P. Tieleman, and S. J. Marrink, "Computational lipidomics with insane: A versatile tool for generating custom membranes for molecular simulations," J. Chem. Theory Comput. **11**, 2144–2155 (2015).
[18]M. J. Abraham, T. Murtola, R. Schulz, S. Páll, J. C. Smith, B. Hess, and E. Lindahl, "GROMACS: High performance molecular simulations through multi-level parallelism from laptops to supercomputers," SoftwareX **1-2**, 19–25 (2015).
[19]G. Bussi, D. Donadio, and M. Parrinello, "Canonical sampling through velocity rescaling," J. Chem. Phys. **126**, 014101 (2007).
[20]M. Parrinello and A. Rahman, "Polymorphic transitions in single crystals: A new molecular dynamics method," J. Appl. Phys. **52**, 7182–7190 (1981).
[21]W. Humphrey, A. Dalke, and K. Schulten, "VMD – Visual molecular dynamics," J. Mol. Graphics **14**, 33–38 (1996).
[22]H. J. C. Berendsen, J. P. M. Postma, W. F. van Gunsteren, A. DiNola, and J. R. Haak, "Molecular dynamics with coupling to an external bath," J. Chem. Phys. **81**, 3684–3690 (1984).
[23]J. T. Bullerjahn, S. von Bülow, and G. Hummer, "Optimal estimates of self-diffusion coefficients from molecular dynamics simulations," J. Chem. Phys. **153**, 024116 (2020).
[24]See https://github.com/bio-phys/DiffusionGLS for diffusion coefficient fitting.
[25]S. von Bülow, J. T. Bullerjahn, and G. Hummer, "Systematic errors in diffusion coefficients from long-time molecular dynamics simulations at constant pressure," J. Chem. Phys. **153**, 021101 (2020).
[26]See https://github.com/jhenin/qwrap for qwrap — Fast PBC wrapping and unwrapping for VMD.
[27]S. Buchoux, "FATSLiM: A fast and robust software to analyze MD simulations of membranes," Bioinformatics **33**, 133–134 (2017).
[28]Q. Waheed and O. Edholm, "Undulation contributions to the area compressibility in lipid bilayer simulations," Biophys. J. **97**, 2754–2760 (2009).
[29]P. Ben Ishai, E. Mamontov, J. D. Nickels, and A. P. Sokolov, "Influence of ions on water diffusion—A neutron scattering study," J. Phys. Chem. B **117**, 7724–7728 (2013).
[30]J. F. Nagle and S. Tristram-Nagle, "Structure of lipid bilayers," Biochim. Biophys. Acta, Rev. Biomembr. **1469**, 159–195 (2000).
[31]R. M. Venable, F. L. H. Brown, and R. W. Pastor, "Mechanical properties of lipid bilayers from molecular dynamics simulation," Chem. Phys. Lipids **192**, 60–74 (2015).
[32]M. Saeedimasine, A. Montanino, S. Kleiven, and A. Villa, "Role of lipid composition on the structural and mechanical features of axonal membranes: A molecular simulation study," Sci. Rep. **9**, 8000–8012 (2019).
[33]H. I. Ingólfsson, M. N. Melo, F. J. Van Eerden, C. Arnarez, C. A. Lopez, T. A. Wassenaar, X. Periole, A. H. De Vries, D. P. Tieleman, and S. J. Marrink, "Lipid organization of the plasma membrane," J. Am. Chem. Soc. **136**, 14554–14559 (2014).
[34]A. Catte, M. Girych, M. Javanainen, C. Loison, J. Melcr, M. S. Miettinen, L. Monticelli, J. Määttä, V. S. Oganesyan, O. H. S. Ollila *et al.*, "Molecular electrometer and binding of cations to phospholipid bilayers," Phys. Chem. Chem. Phys. **18**, 32560–32569 (2016).
[35]L. Borges-Araújo, P. C. T. Souza, F. Fernandes, and M. N. Melo, "Improved parameterization of phosphatidylinositide lipid headgroups for the Martini 3 coarse-grain force field," J. Chem. Theory Comput. **18**, 357–373 (2021).
[36]M. Winger, D. Trzesniak, R. Baron, and Wf. van Gunsteren, "On using a too large integration time step in molecular dynamics simulations of coarse-grained molecular models," Phys. Chem. Chem. Phys. **11**, 1934–1941 (2009).
[37]S. Piana, A. G. Donchev, P. Robustelli, and D. E. Shaw, "Water dispersion interactions strongly influence simulated structural properties of disordered protein states," J. Phys. Chem. B **119**, 5113–5123 (2015).
[38]R. Alessandri, P. C. T. Souza, S. Thallmair, M. N. Melo, A. H. De Vries, and S. J. Marrink, "Pitfalls of the Martini model," J. Chem. Theory Comput. **15**, 5448–5460 (2019).
[39]H. Oberhofer and C. Dellago, "Large time-step, fast-switching free energy calculations with non-symplectic integrators," Isr. J. Chem. **47**, 215–223 (2007).
[40]L. I. Vazquez-Salazar, M. Selle, A. H. De Vries, S. J. Marrink, and P. C. T. Souza, "Martini coarse-grained models of imidazolium-based ionic liquids: From nanostructural organization to liquid–liquid extraction," Green Chem. **22**, 7376–7386 (2020).
[41]P. Vainikka, S. Thallmair, P. C. T. Souza, and S. J. Marrink, "Martini 3 coarse-grained model for type III deep eutectic solvents: Thermodynamic, structural, and extraction properties," ACS Sustainable Chem. Eng. **9**, 17338–17350 (2021).
[42]S. Baoukina, D. Rozmanov, and D. P. Tieleman, "Composition fluctuations in lipid bilayers," Biophys. J. **113**, 2750–2761 (2017).
[43]S. Thallmair, M. Javanainen, B. Fábián, H. Martinez-Seara, and S. J. Marrink, "Nonconverged constraints cause artificial temperature gradients in lipid bilayer simulations," J. Phys. Chem. B **125**, 9537–9546 (2021).